ACS APPLIED MATERIALS & INTERFACES

Research Article

Cite This: ACS Appl. Mater. Interfaces XXXX, XXX, XXX−XXX

www.acsami.org

Oxygen-Insensitive Aggregates of Pt(II) Complexes as Phosphorescent Labels of Proteins with Luminescence Lifetime-Based Readouts

Pietro Delcanale,[†,#] Anzhela Galstyan,[‡] Constantin G. Daniliuc,[§] Hernan E. Grecco,[∥] Stefania Abbruzzetti,[†] Andreas Faust,[⊥] Cristiano Viappiani,*[,†] and Cristian A. Strassert*[,‡]

[†]Dipartimento di Scienze Matematiche, Fisiche e Informatiche, Parco Area delle Scienze 7A, 43124 Parma, Italy

[‡]Physikalisches Institut and Center for Nanotechnology, Westfälische Wilhelms-Universität Münster, Heisenbergstraße 11, D-48149 Münster, Germany

[§]Organisch-Chemisches Institut, Westfälische Wilhelms-Universität Münster, Corrensstraße 40, D-48149 Münster, Germany

[∥]Departamento de Física, FCEyN, UBA and IFIBA, CONICET, Pabellón 1, Ciudad Universitaria, 1428 Buenos Aires, Argentina

[⊥]University Hospital Münster and European Institute for Molecular Imaging, Westfälische Wilhelms-Universität Münster, Waldeyerstraße 15, D-48149 Münster, Germany

Supporting Information

ABSTRACT: The synthesis and photophysical properties of a tailored Pt(II) complex are presented. The phosphorescence of its monomeric species in homogeneous solutions is quenched by interaction with the solvent and therefore absent even upon deoxygenation. However, aggregation-induced shielding from the environment and suppression of rotovibrational degrees of freedom trigger a phosphorescence turn-on that is not suppressed by molecular oxygen, despite possessing an excited-state lifetime ranging in the microsecond scale. Thus, the photoinduced production of reactive oxygen species is avoided by the suppression of diffusion-controlled Dexter-type energy transfer to triplet molecular oxygen. These aggregates emit with the characteristic green luminescence profile of monomeric complexes, indicating that Pt−Pt or excimeric interactions are negligible. Herein, we show that these aggregates can be used to label a model biomolecule (bovine serum albumin) with a microsecond-range luminescence. The protein stabilizes the aggregates, acting as a carrier in aqueous environments. Despite spectral overlaps, the green phosphorescence can be separated by time-gated detection from the dominant autofluorescence of the protein arising from a covalently bound green fluorophore that emits in the nanosecond range. Interestingly, the aggregates also acted as energy donors able to sensitize the emission of a fraction of the fluorophores bound to the protein. This resulted in a microsecond-range luminescence of the fluorescent acceptors and a shortening of the excited-state lifetime of the phosphorescent aggregates. The process that can be traced by a 1000-fold increase in the acceptor's lifetime mirrors the donor's triplet character. The implications for phosphorescence lifetime imaging are discussed.

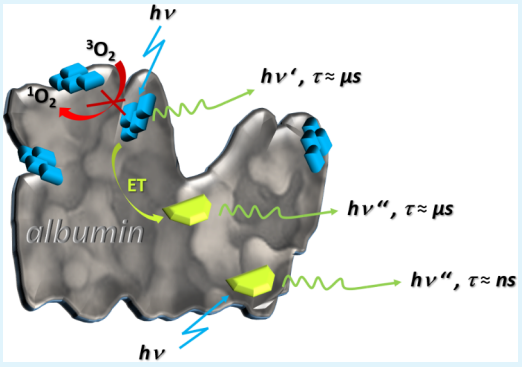

KEYWORDS: *Pt(II) complex, energy transfer, donor−acceptor, PLIM, spectroscopy, photophysics, labeling, time-gated spectroscopy*

INTRODUCTION

Coordination compounds able to emit from the excited triplet state have found applications in molecular bioimaging. Among these, species with d^6 and d^8 electronic configurations have been described, including Re(I), Pt(II), and Ir(III) complexes.[1−5] Such transition-metal complexes are usually quenched upon aggregation because of triplet−triplet annihilation processes, which become more probable for longer excited-state lifetimes. On the other hand, Pt(II) complexes can stack into luminescent aggregates because of their d^8 electronic configuration, which leads to planar coordination compounds where aggregation favors the interaction between d_{z^2} orbitals protruding out of the molecular plane. If compared with the monomeric units, this usually leads to a red-shifted emission arising from the aggregated species with excimeric and metal−metal-to-ligand charge-transfer character. Thus, supramolecular arrays displaying strong phosphorescence are obtained. The abovementioned coordination compounds possess a defined chemical structure without dissociation equilibria, which facilitates their purification, characterization, processability, and conjugation with targeting units. Their long triplet-state lifetimes (in the microsecond range) are particularly useful in

Received: February 13, 2018
Accepted: June 19, 2018

DOI: 10.1021/acsami.8b02709
ACS Appl. Mater. Interfaces XXXX, XXX, XXX−XXX

Scheme 1. Schematic Representation of the Controlled Aggregation of Pt(II) Complexes (Blue) at Fluorescein-Labeled BSA (Gray with Green Labels)[a]

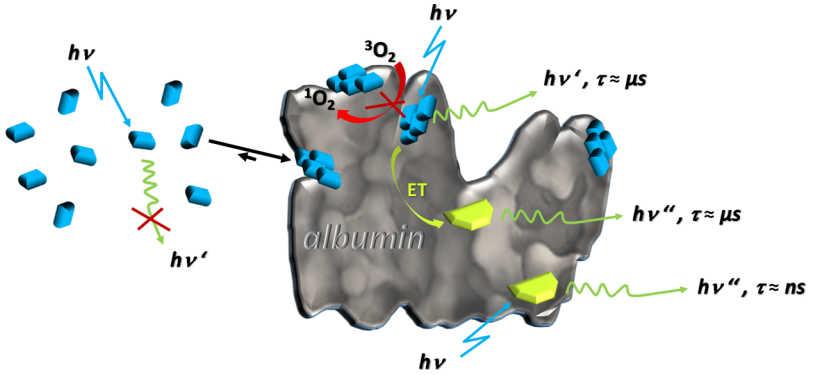

[a]Although the monomeric species are not phosphorescent (left), the aggregates formed at the protein (right) can emit in the microsecond range and sensitize the luminescence of fluorescein via ET. Thus, the emission lifetime of fluorescein is shifted from nanoseconds to microseconds. The aggregated complexes are not quenched by molecular oxygen

bioimaging applications as it enables the suppression by the time-gated imaging of the autofluorescence of the sample (in the nanosecond range). However, their long-lived triplet states are also prone to luminescence quenching and lifetime shortening by energy transfer (ET) to triplet molecular oxygen, which is accompanied in turn by the photoproduction of reactive oxygen species (ROS) such as singlet molecular oxygen. Even though the photoproduction of ROS could be used for phototherapy, it limits the applicability for bioimaging as the mere observation affects signaling processes and causes unwanted photodamage of biological structures.[6] On the other hand, their oxygen sensitivity can also be used to monitor the concentration of molecular oxygen. For example, it is possible to detect hypoxic tissues from the prolonged excited lifetimes or enhanced luminescence quantum yield. Because they usually absorb in the deep blue or UV range of the electromagnetic spectrum, a two-photon excitation in the near-infrared (NIR) region has been proposed to avoid the damage to biological structures and low penetration depth into tissues associated with short-wavelength radiation.[7]

Lanthanide complexes, on the other hand, display a sharp emission in the visible and in the NIR regions, even though they require polydentate chelating ligands with UV−vis-absorbing antennae to sensitize their photoluminescence, as their direct optical excitation is Laporte-forbidden. Despite possessing excited-state lifetimes ranging in the microsecond to millisecond range, the nature of the inner-shell radiative transitions makes them insensitive to oxygen, whereas the parity-forbidden radiative relaxation negatively affects their intrinsic quantum yields. Moreover, they can undergo dissociation equilibria or coordinate solvent molecules from the environment, which shortens their excited-state lifetimes while drastically dropping their generally low photoluminescence quantum yields.[8]

Phosphorescence lifetime imaging microscopy (PLIM)[9−13] has become increasingly investigated as an alternative to fluorescence lifetime imaging microscopy (FLIM)[14] to investigate molecular interactions and conformational changes. The molecular resolution of typical FLIM assays is limited mainly by their temporal resolution in relation to the lifetime and the number of photons that can be collected in a given time. For a given experimental system and duration, a longer lifetime yields a better relative temporal resolution but a smaller number of photons. Although the optimal compromise depends on the particular system, the use of long triplet lifetimes could be especially useful when a small change in the transfer efficiency is expected. In FLIM, such a change could lead to a sub-nanosecond lifetime changes, like the temporal resolution of typical detection systems. In contrast, a 1000-fold increase (from nanosecond to microsecond) in the excited-state lifetime as typically found in PLIM would boost such a change providing a higher sensitivity. ET from a triplet state is usually expected to be inefficient because of the low radiative rate constants associated with phosphorescence. Nonetheless, if late transition-metal ions with strong ligand-field splitting are coordinated to luminophoric chelates that enable metal-to-ligand or ligand-to-metal charge-transfer excitations, a strong spin−orbit coupling mixes singlet-state character into the triplet states promoting fast intersystem crossing and up to 100% phosphorescence quantum yield. However, the implementation of triplet emitters would require the absence of quenching by molecular oxygen and therefore excluding monomeric triplet emitters based on transition-metal complexes.

In our previous work, we have shown that Pt(II) complexes bearing dianionic tridentate luminophores can be used as (electro)luminescent monomers[15] or self-assembled fibers[16−18] and crystals.[19] Two-dimensional confinement at semiconducting and metallic interfaces allowed us to track intermetallic interactions by scanning tunneling microscopy,[20,21] X-ray photoelectron spectroscopy, and luminescence microscopy.[22] This knowledge allowed us to tune the luminescence of the monomeric species from green to blue by setting submolecular setscrews,[23] whereas the emission of the aggregated species was shifted into the deep red portion of the electromagnetic spectrum by varying the Pt−Pt distance as an intermolecular tuning tool.[24] Recently, we have shown that the supramolecular polymeric arrays doped with Pt(II) complexes can be dispersed in aqueous environments without diffusional quenching by molecular oxygen.[25] In this paper, we describe a new tailored Pt(II) complex that does not emit as a monomer even in the absence of oxygen but is able to form phosphorescent aggregates that show no Pt−Pt interaction while being insensitive to quenching by molecular oxygen (Scheme 1). We investigated its capability for time-gated detection by inducing a controlled aggregation on a

DOI: 10.1021/acsami.8b02709
ACS Appl. Mater. Interfaces XXXX, XXX, XXX−XXX

biomolecular model [in this case, fluorescein-labeled bovine serum albumin (BSA)]. We finally described the ET from the phosphorescent aggregates to a fraction of the fluorescent labels at the protein.

RESULTS AND DISCUSSION

Synthesis and Structural Properties. The tridentate luminophore was synthesized according to a literature procedure.[26] Complexation with an appropriate Pt(II) precursor led to the required complex, according to our previously established methodology and as described in the Supporting Information.[27] The resulting complex (Figure 1)

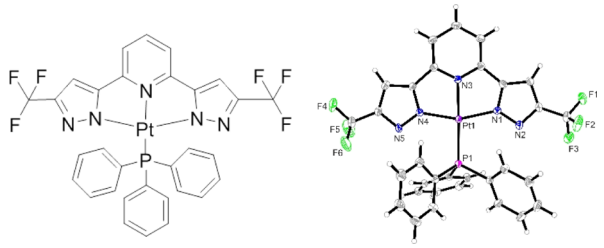

Figure 1. Chemical structure of the herein employed complex (**AG97**) as obtained by X-ray diffractometry analysis. Thermal ellipsoids are shown with 30% probability.

was characterized by high-resolution mass spectrometry analysis and NMR spectroscopy techniques (Figures S1–S3). Suitable crystals for X-ray diffractometry analysis were obtained, showing a practically square-planar coordination environment where the bulky triphenylphosphine ligand clearly protrudes out of the coordination plane, thus avoiding Pt–Pt interactions in the crystals (Table S1 and Figures S4–S7). According to our previous work, an irreversible binding to the Pt(II) center of tridentate luminophores and the monodentate ancillary ligand is expected, withstanding hydrolysis and high sublimation temperatures.

Photophysical Characterization. **AG97** is characterized by a quasi-square-planar coordination of the metal center and a mainly hydrophobic structure, which is responsible for the extensive aggregation of the compound in aqueous environments. **AG97** readily dissolves in common organic solvents such as dichloromethane (DCM) or dimethyl sulfoxide (DMSO), where it shows structured absorption bands centered at around 340 and 400 nm (Figures 2 and S8), which can be attributed to transitions into singlet ligand-centered (^{1}LC) and singlet metal-to-ligand charge-transfer (^{1}MLCT) states. The absorption spectrum is mirrored in the excitation spectrum (Figure S9), and the emission shows a clearly structured profile that can be attributed to the vibrational progression associated with the emission from a metal-perturbed LC triplet state. At 77 K in a frozen glassy matrix (where solvent reorientation is suppressed and the MLCT states are destabilized, leading to a reduced metal participation in the mainly LC emissive state), a minor blue shift is observed, whereas the vibrational progression is more pronounced because of the reduced interaction with the environment (Figure S10). The excited-state lifetimes in fluid organic solvents at room temperature are surprisingly short for a triplet emitter (around 15 ns) and therefore insensitive to dissolved oxygen and deoxygenation (Figures S11 and S12). In the frozen matrix at 77 K, however, a monoexponential decay in the microsecond range is recovered (19 μs, Figure S13). We therefore attribute the shortened luminescence decay in a fluid solution to a strong coupling with the solvent (physical quenching). The absorption spectrum of **AG97** in phosphate-buffered saline (PBS) buffer, whose pH and ionic strength are biologically relevant because they closely match the conditions found in tissues, displays the typical features of molecular aggregates: broadened and poorly structured absorption bands; a red-shifted main band centered at 350 nm, that is, 10 nm shifted with respect to an equimolar DMSO solution (Figure 2); and an intense background exponentially growing at

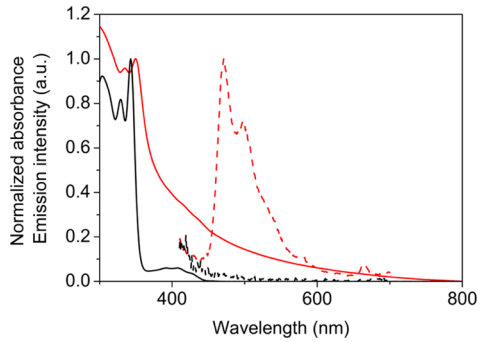

Figure 2. Normalized absorption (solid) and emission (dashed) spectra for **AG97** in PBS buffer (red) and DMSO (black). Absorption spectra are normalized for the peak value, and emission spectra are normalized for a peak value of **AG97** in PBS. T = 20°C, λ_{exc}= 350 or 340 nm.

shorter wavelengths, which does not reflect the absorption of photons but arises from a Rayleigh-like scattering of the incident light owing to the presence of large molecular aggregates (Figure 2). Hydrophobic aggregation is generally known to promote nonradiative processes of de-excitation, thus impairing photoluminescence. Surprisingly, **AG97** behaves differently because its emission appears to be promoted by the formation of aggregates. In fact, the complex's photoluminescence is completely quenched in DMSO (Figure 2) and also extremely weak in DCM, where the compound is well-soluble. Conversely, a clear structured emission (luminescence quantum yield ~0.05) is obtained from **AG97** aggregates in PBS buffer, with two main bands centered at around 470 and 497 nm (Figure 2). A specific mechanism of chemical quenching induced by organic solvents appears unlikely because the observed spectroscopic properties are very similar in both the organic solvents tested herein (DMSO and DCM). The physical phenomena appear more likely to explain the increased emission of **AG97** occurring from aggregates with respect to monomers in homogeneous solution and are probably due to several concomitant effects: an increased rigidity of the molecules within the aggregate; a shielding from solvent and oxygen; and a weak coupling within the aggregates because of the rather bulky ancillary ligand. An important consequence of this unexpected behavior is that the photoluminescence can be conveniently regarded as an experimental tool to monitor the extent of the aggregation because monomers can be considered as nonemissive species. This is exactly opposite to the behavior observed for many hydrophobic photoactive dyes: usually, hydrophobic aggregates are negligibly fluorescent while the monomeric species (in organic solvents or bound to solubilizing structures) recover the ability of fluorescence emission, which can be used as a tool to determine the binding constant.[28] Aggregation-induced

DOI: 10.1021/acsami.8b02709
ACS Appl. Mater. Interfaces XXXX, XXX, XXX–XXX

Table 1. Spectroscopic Properties of 3 μM AG97 in Different Solvents[a]

	air-equilibrated		deoxygenated	
solvent	τ_1	τ_2	τ_1	τ_2
PBS	(0.9 ± 0.2) μs, 39%	(3.0 ± 0.3) μs, 61%	(0.73 ± 0.09) μs, 35%	(2.9 ± 0.3) μs, 65%
DCM	(5.8 ± 0.1) ns, 32%	(15.7 ± 0.1) ns, 68%	(5.1 ± 0.1) ns, 27%	(14.0 ± 0.5) ns, 73%

[a] τ are the lifetimes and quantum yields of photoluminescence, respectively (λ_{exc} = 350 nm or 340 nm; λ_{em} = 470 nm; T = 20°C); deoxygenation was achieved in the solution with a moderate flow of pre-equilibrated argon for 20 min.

emission caused by the suppression of rotovibrational degrees of freedom has been described in the literature.[29−31] We have recently shown that metal−organic aggregates can show such a behavior with[16−18] or without[32] intermetallic interactions and participation of heavy atoms in the emissive states, whereas purely organic push−pull luminophores can yield both fluorescent and phosphorescent aggregates[31] that are useful to label bacteria.[33]

As discussed above, the hydrophobic aggregation of **AG97** does not preclude the photoluminescence upon injection into aqueous phases such as PBS buffer. However, both its emission spectra and its luminescence decays are characterized by a large variability. Additionally, the intensity of emission in the aqueous buffer shows an ∼20% decrease within 10−30 min after the preparation of the sample and is roughly stable only for a few hours. This is likely a consequence of multiple aggregation equilibria rather than a chemical degradation and constitutes a limitation for the pure complex in aqueous environments. Despite being affected by a rather large experimental uncertainty, the photoluminescence decays for pure **AG97** in PBS buffer yielded lifetime values on the order of few microseconds (Table 1), as observed for similar triplet emitters.[18,34] The photoluminescence quantum yield in PBS is 0.05 and does not vary upon deoxygenation. As mentioned above, the measured lifetime values decrease by roughly 2 orders of magnitude in fluid organic solvents at room temperature where the emission is barely detectable, and aggregation can be neglected (Table 1).

A notable feature of **AG97** is the substantial insensitivity of its photophysical properties to variations in the concentration of molecular oxygen (O_2) (Table 1). Even an extended purging with argon does not affect any photophysical parameter of **AG97** in different solvents. For the suspension in PBS, the argon bubbling just induced an apparent degradation and luminescence decrease of the aggregates but without affecting the spectroscopic parameters such as quantum yields and lifetimes. This observed insensitivity of the photophysics to O_2 is rather unexpected, particularly considering the triplet character of the molecule's excited state. A plausible hypothesis is that the **AG97** molecules embedded in the aggregates are shielded from the environment (solvent and O_2) and that no detectable change is observed upon deoxygenation. For the purposes of this work, it is important to point out that in biologically relevant conditions, for example, in PBS solution, there is no spectroscopic evidence for the sensitivity of the complex toward O_2 and that the long-lived decay of photoluminescence emission arising from a microsecond-lived triplet is not affected by the O_2 concentration. In fluid organic solvents, the oxygen insensitivity is likely a consequence of the fast depopulation of the molecule's excited state through nonradiative processes that dominate over other deactivation mechanisms.

Interaction of AG97 with BSA. A carrier system able to stabilize the properties of the triplet emitter in biological conditions appears essential for the applications of **AG97** in molecular imaging. Our previous results obtained with other hydrophobic photoactive ligands showed that proteins are good carrier systems because they are water-soluble, homogeneous, biocompatible, and able to bind and transport the ligand at specific binding sites.[28,35] We chose BSA as the model carrier because it constitutes a widespread protein able to interact with a wide range of chemically different molecules and is essential for the understanding of the pharmacokinetics of drugs.[36] Binding of hydrophobic dyes to proteins is often assessed spectroscopically by monitoring the changes in absorption and emission spectra in the presence of the carrier protein.[28,35]

Figure 3 shows the changes in absorption and emission spectra of a 3 μM BSA solution at increasing concentrations of

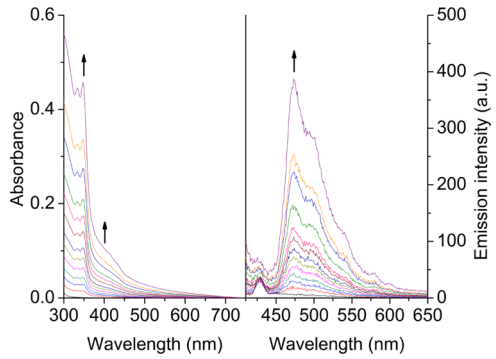

Figure 3. Absorption (left) and emission (right) spectra for PBS buffer solution containing 3 μM BSA titrated with increasing concentrations of **AG97** (from 0 to 20 μM). The arrows indicate the direction of increasing concentration.

AG97 (from 0 to 20 μM). An identical titration conducted in the absence of BSA (Figure S14) shows higher background scattering because of lack of interaction with the protein. The lower scattering in the presence of BSA shows that aggregation of **AG97** is controlled by hydrophobic interactions with the protein, which acts as a template. Additional information about the complex aggregated at the protein can be obtained from time-resolved luminescence decays: Figure 4 summarizes the results obtained from the analysis of the decay fittings, which were well described with a biexponential fitting model. The histogram of Figure 4 shows the good reproducibility of the decay parameters in the presence of BSA at different concentrations of **AG97**. Conversely, the results obtained in the absence of protein in pure buffer (Figure S15) appear scattered and are characterized by a systematic increase of the lifetime values at higher concentrations of **AG97** because of the growth of larger yet irregular aggregates. The average values from data in Figure 4 are $\langle\tau_1\rangle$ = (0.28 ± 0.05) μs (∼57%) and $\langle\tau_2\rangle$ = (0.91 ± 0.06) μs (∼43%). The corresponding average lifetime values in pure PBS are longer

DOI: 10.1021/acsami.8b02709
ACS Appl. Mater. Interfaces XXXX, XXX, XXX−XXX

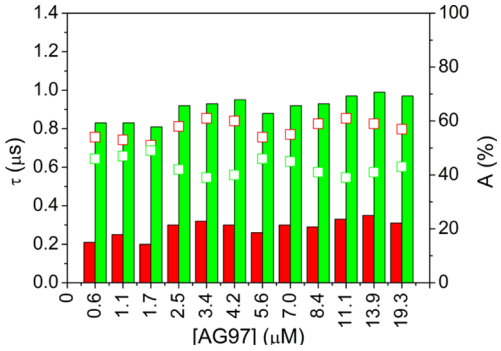

Figure 4. Lifetime values τ_1 (red bar) and τ_2 (green bar) and respective relative amplitude-weighted pre-exponential factors A_1 (red empty squares) and A_2 (green empty squares) at increasing **AG97** concentrations in PBS buffer with 3 μM BSA. λ_{exc} = 375 nm, λ_{em} = 465 nm.

and carry a larger uncertainty than in the presence of the protein: $\langle\tau_1\rangle$ = (0.6 ± 0.2) μs (~70%) and $\langle\tau_2\rangle$ = (2.4 ± 0.4) μs (~30%). The shorter lifetimes in the presence of BSA are consistent with the reduced Φ_{em} (0.02) obtained with a large excess of BSA, if compared with pure PBS buffer (Φ_{em} = 0.05). This shortening of the lifetimes and reduction of Φ_{em} indicate an interaction between **AG97** and BSA, even though the absorption and emission bands appear essentially unaltered by the protein (Figures 3 and S13). The results also show that **AG97** molecules sense similar environment upon aggregation in pure PBS and in the presence of albumin. Thus, a homogeneous population of small, weakly scattering clusters of **AG97** is stabilized by the interaction with BSA, as inferred from the consistency and reproducibility of the spectroscopic data. The reduction of luminescence quantum yields and decay lifetimes in the presence of BSA points to smaller clusters than in pure buffer with reduced shielding from the solvent. However, a direct quenching by the protein cannot be excluded, for instance, by electron transfer.

As reported above for **AG97** in pure buffer, no changes in the photophysical properties are detected upon deoxygenation of solutions containing **AG97** and BSA, which is particularly true regarding the emission lifetimes (Figure 5). This fact supports the hypothesis that the interaction with BSA involves small clusters of **AG97**, whose properties are not affected by oxygen removal, as opposed to oxygen-sensitive monomers. A

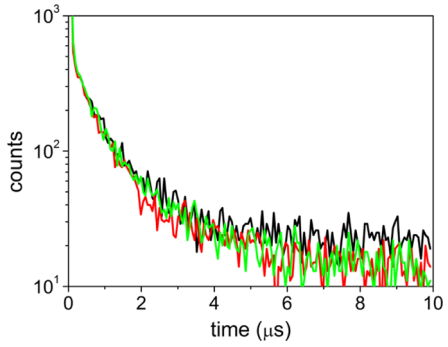

Figure 5. Time-resolved luminescence decay (λ_{exc} = 370 nm, λ_{em} = 470 nm, T = 20°C) for 100 μM BSA with 2.5 μM **AG97** in PBS buffer air-equilibrated (black) and after gentle purging with pre-equilibrated argon for 60 min (red) and 120 min (green). The shortest times are cut because they are affected by intense scattered light.

large excess of BSA was used in the deoxygenation experiments to ensure that the majority of **AG97** interacts with the protein, with negligible contribution of unbound molecules. Thus, it is possible to conclude that **AG97** adsorbed onto BSA: (I) is spectroscopically reproducible; (II) retains a luminescence emission on the microsecond time scale with a clearly detectable intensity; and (III) possesses an excited state that does not show any traceable sensitivity toward O_2. This is particularly interesting because the photoexcited states of similar molecules, having a triplet character, often form exciplexes with O_2 producing cytotoxic reactive oxygen species.[34,37] The system thus appears to have an elevated level of biocompatibility and shows potential as a photoluminescent probe for bioimaging without the formation of reactive oxygen species.

Colabeling of BSA with Fluorescein Isothiocyanate and AG97. A relevant issue when performing experiments based on fluorescence detection in biological samples, for example, organelles, cells, or tissues, is to distinguish the emission of the fluorescent probe from background noise and from the sample's autofluorescence.[38−41] The complex **AG97** conjugated with BSA has luminescence lifetimes that are 2−3 orders of magnitude longer than the typical fluorescence decays. This enables an experimental discrimination of the **AG97** emission from any fluorescence, autofluorescence, or scattering contribution simply by introducing a temporal gating on the time-resolved signal.[42,43] In our study, BSA was covalently labeled with the fluorophore fluorescein isothiocyanate (FITC) to simulate an intense autofluorescence. The labeled protein (BSAFITC) was easily obtained with a standard procedure in PBS buffer.[44] The binding of FITC to the aminoacidic moieties was confirmed by a 6 nm red shift in the absorption and emission spectra. Also, a change in the fluorescence decay of fluorescein was observed after the conjugation: a biexponential model with τ_1 = 2 ns (15%) and τ_2 = 4 ns (85%) well-fitted the decay for free FITC in PBS, whereas the triexponential decay was necessary for BSAFITC, namely, τ_1 = 0.2 ns (41%), τ_2 = 1.3 ns (26%), and τ_3 = 4.0 ns (33%).

There is no spectroscopic evidence that labeling the protein with FITC significantly affects the interaction with **AG97**. The same considerations made for the unlabeled protein (i.e., the reduced scattering of light and shortened emission lifetimes with respect to the **AG97** in PBS) also hold true for **AG97** in the presence of BSAFITC. The labeling of the protein with FITC is a particularly convenient method because both emitting species, that is, fluorescein and **AG97**, can be clearly distinguished experimentally by exploiting the different spectral region and the different time scale of their emission. The absorption and emission spectra of both luminophores bound to BSA are shown in Figure 6, where three main spectral regions can be identified:

(I) BSA-bound **AG97** exhibits a main emission band centered at 470 nm (solid cyan), that is, in a region where BSAFITC does not emit (solid green). Thus, the luminescence of the Pt complex can be selectively detected by setting the emission wavelength at ~470 nm. (II) In the spectral region between 490 and ~570 nm, the emission of both the species overlaps (solid cyan and green). Pure BSAFITC shows the main emission band centered at 525 nm (green) and its fluorescence occurs with high quantum yield (close to unity[45]) on a time scale of a few nanoseconds. Conversely, protein-bound **AG97** (cyan) exhibits a weaker emission than

DOI: 10.1021/acsami.8b02709
ACS Appl. Mater. Interfaces XXXX, XXX, XXX−XXX

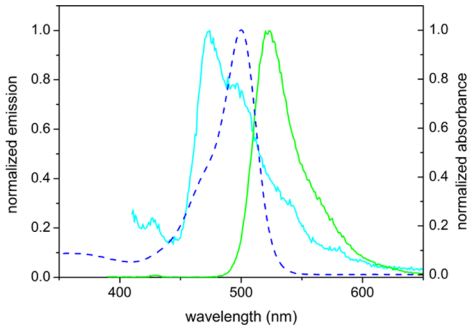

Figure 6. Emission spectrum of **AG97** bound to BSA (cyan solid, λ_{ex} = 375 nm), compared to the absorption (blue dashed) and emission (green solid, λ_{ex} = 490 nm) spectra of BSAFITC. Spectra are normalized at the maximum value.

BSAFITC, but occurring on a longer time scale, in the order of microseconds. Thus, the experimental discrimination of the two species in this spectral region can only occur on a timely basis. (III) At longer wavelengths (>570 nm), the luminescence emission of **AG97** becomes negligible and only the much more intense fluorescence of BSAFITC is relevant.

A solution of BSAFITC in PBS was titrated with an increasing concentration of **AG97**, from 0 to ~20 μM. The resulting absorption spectra are reported in the left panel of Figure 7, where the strong absorption band of fluorescein

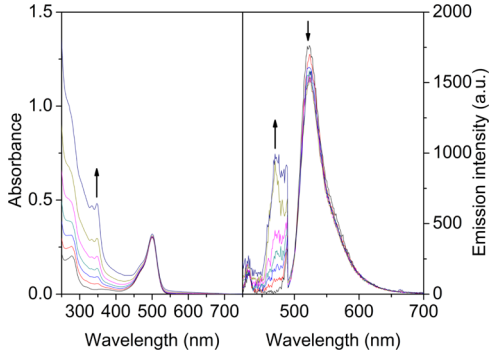

Figure 7. Absorption (left) and emission (right) spectra obtained for the titration of BSAFITC (3 μM) in PBS at increasing **AG97** concentrations (from 0 to 20 μM). λ_{ex} = 375 nm, T = 20°C. The emission data in the 420−490 nm range reported in the right plot are shown on a ×10 scale. The arrows indicate the direction of increasing concentration.

centered at 500 nm can be observed. As for BSA, the presence of the labeled protein limits the aggregation of the Pt(II) complex in PBS, thus reducing the background because of light scattering by larger aggregates. The corresponding emission spectra are reported in the right panel of Figure 7, where the intense fluorescence band of fluorescein can be recognized at 525 nm (compare with Figure S17, where the absorption and emission spectra of an isoabsorptive FITC solution in PBS are titrated with the complex). When the concentration of **AG97** is increased, its emission band at 470 nm can be measured (upward arrow in the right panel of Figure 7), even if it remains considerably lower than the emission from the fluorophore. The lowered intensity of the fluorescein emission band at increasing concentrations of **AG97** is attributed to the inner filter effect because of light scattering induced by the aggregates (the effect is more prominent in the absence of BSA, where larger aggregates are present, see Figure S17). In the spectral region where the emissions of the two species overlap, that is, between 490 and 570 nm, the steady-state spectra shown in the right panel of Figure 7 do not allow a distinction of the weak luminescence of **AG97** hidden behind the intense fluorescence of BSAFITC. This model simulates a condition often met in biological samples, that is, when unwanted autofluorescence contributions dominate over the emission of the luminescent reporter. The easiest way to experimentally isolate the **AG97** emission would be to set the detection wavelength sharply at 470 nm where fluorescein does not emit. However, in real samples, autofluorescence may be intense at this wavelength because of the emission of common endogenous fluorophores such as NADH or flavins.[8]

Selective detection of **AG97** luminescence in the presence of an intense background fluorescence can be achieved by time-gated detection. Figure 8 reports the gated emission spectra

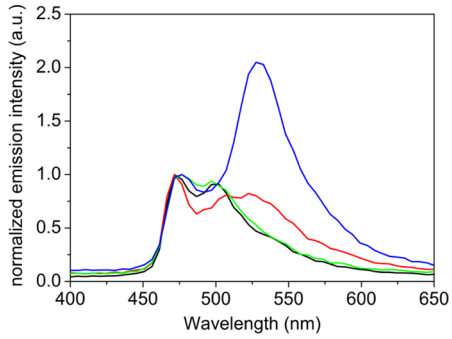

Figure 8. Normalized gated emission spectra obtained for 20 μM solutions of **AG97** in pure PBS buffer (black line) and in the presence of FITC (red line), 2.5 μM BSA (green line), or 2.5 μM BSAFITC (blue line). Gated spectra were collected by pulsed laser excitation at 375 nm with MCS acquisition mode, T = 20°C. The time-resolved signal was integrated in the range 128 ns to 8 μs to obtain the gated spectra. The spectra are normalized to the peak emission of **AG97** at 471 nm. The concentration of free FITC was adjusted to match the peak absorption of the BSAFITC solution, to ensure that the relative concentrations of fluorophores are comparable.

collected for 20 μM **AG97** solutions in PBS buffer (black curve) and in the presence of free FITC (red line), BSA (green line), or BSAFITC (blue line). The spectra were acquired with the same temporal gating at every detection wavelength: the fluorescence emission occurring on the shorter time scale (<128 ns) was discarded, whereas the signal occurring on the longer time scale (128 ns to 8 μs) was integrated to give the shown spectra. After the gated removal of the fluorescence, the shape of the emission spectra for **AG97** in pure PBS buffer (black curve in Figure 8) or with BSA (green curve in Figure 8) is perfectly consistent with that obtained with the usual steady-state detection (Figure 3). Gated spectra are less resolved than the steady-state counterparts, given the 5 nm spacing of the data, which is necessary to reduce the acquisition times. We emphasize that for the gated spectra of **AG97** in the presence of free FITC or BSAFITC, the emission band of **AG97** can be significantly better discriminated than in the corresponding steady-state spectra (Figure 7). However, it is noticeable that a residual contribution of fluorescein emission is still present in the gated spectra and features the typical band at 525 nm. This is particularly evident in the presence of BSAFITC, where the emission band due to the fluorophore is more intense than the one of **AG97**, centered at

DOI: 10.1021/acsami.8b02709
ACS Appl. Mater. Interfaces XXXX, XXX, XXX−XXX

Table 2. Lifetime Values from Fitting with a Biexponential Model (λ_{exc} = 375 nm, T = 20°C, MCS Mode with 32 ns Resolution)[a]

	BSA + AG97		BSAFITC + AG97	
λ_{em}(nm)	$\langle\tau\rangle$	$\langle\tau_2\rangle$	$\langle\tau_1\rangle$	$\langle\tau_2\rangle$
470	(0.28 ± 0.05) μs, 57%	(0.91 ± 0.06) μs, 43%	(0.21 ± 0.03) μs, 57%	(0.76 ± 0.03) μs, 43%
600			(0.14 ± 0.02) μs, 67%	(0.63 ± 0.05) μs, 33%

[a]The average values are obtained from the data of titrations of solutions containing BSA or BSAFITC, with increasing concentrations of **AG97**. The same experimental conditions were used in both experiments.

470 nm. Because the lifetimes for both free FITC and BSAFITC are in the order of few nanoseconds, it is excluded that a residual fluorescence can generate such intense bands in the gated spectra. Additionally, when BSAFITC is titrated with increasing concentrations of **AG97** (Figure S16), the extent of the fluorescein luminescence at 525 nm appears to grow along with the **AG97** concentration.

These observations are consistent with the occurrence of an ET between **AG97** (donor) and fluorescein (acceptor), leading to a delayed emission of the fluorophore in the microsecond time scale. In Figure 6, it is possible to see that the emission spectrum of **AG97** and the absorption spectrum of BSAFITC are significantly overlapped so that the condition for the ET is fulfilled. In the case of BSAFITC, the proximity of the phosphorescent donor and the fluorescent acceptor could enable a resonant ET, even though other processes (e.g., emission−absorption or Dexter-like) cannot be fully excluded. The ET between unlinked fluorophores (pure FITC without BSA) and aggregates of the complex is not expected for acceptor concentrations in the 20 μM range as the average donor−acceptor distance would be an order of magnitude larger than the typical Förster range. However, we cannot exclude that free FITC might adsorb onto aggregates of the complex (even in the absence of BSA), leading to a resonant (Förster-like) or other type of ET (e.g., emission−absorption or Dexter-like).

In Table 2, the average values for emission lifetime components obtained with detection at 470 nm (where only **AG97** emits) and at 600 nm (where fluorescein emission is prevailing) are compared for **AG97** in the presence of BSA and BSAFITC. When the fluorophore was present, the fluorescein's emission at 600 nm roughly mirrored the lifetimes of the complex at 470 nm, supporting the idea of ET. Additionally, the slight shortening of **AG97** lifetime components (at 470 nm) in the presence of BSAFITC (compared with BSA solutions) suggests a nontrivial ET to the fluorophore, even though emission−absorption cannot be completely ruled out. On the other hand, a trivial ET (emission−absorption) seems to be operating between aggregates of **AG97** in PBS and free FITC, as no significant lifetime shortening can be traced within the experimental uncertainty (see Table S2). It should be pointed out that we cannot completely exclude that a fraction of free FITC (in the absence of BSA) might adsorb onto the aggregates of the phosphorescent complex, thus favoring the ET processes. From a visual comparison of the intensity of the 525 nm centered emission band in Figure 8, it is easy to recognize that the extent of ET from **AG97** to fluorescein appears more efficient when the fluorophore is attached to the protein (i.e., for BSAFITC) than when it is in the solution. This is consistent with the idea of a transfer promoted by the structure of the protein that offers a scaffold able to keep donor and acceptor spatially close. A quantitative discrimination of resonance ET, radiative ET, or other nonradiative quenching processes induced by the presence of the fluorophore is not possible with this technique and is an object of ongoing investigations.

CONCLUSIONS

We have shown that the choice of the right tridentate luminophore can yield a phosphorescent Pt(II) complex that is dark as a monomeric species but phosphorescent upon aggregation, without quenching by triplet molecular oxygen and without ROS photoproduction. These aggregates can be used to label biomolecules and separated from background fluorescence by time-gated detection. Moreover, they can act as donors for ET in lifetime imaging, providing a 1000-fold enhancement of the fluorescent acceptor's lifetime, which is particularly convenient for monitoring living systems. In the future, metabolic trapping and accumulation of such phosphorescent species could also be monitored based on phosphorescence turn-on. We are presently synthesizing analogous complexes with reactive groups for covalent binding to biomolecules such as proteins, sugars, and nucleic acids, facilitated by the modification of the modular ancillary ligand. The two-photon excitation facilitated by the excited state's charge-transfer character may overcome the UV absorption of these species, whereas their use in super-resolution microscopy is an object of current investigations.

EXPERIMENTAL SECTION

Details regarding the synthetic procedures and spectroscopic methods can be found in the electronic Supporting Information.

ASSOCIATED CONTENT

Supporting Information

The Supporting Information is available free of charge on the ACS Publications website at DOI: 10.1021/acsami.8b02709.

Experimental details and further information regarding synthesis, characterization, X-ray diffractometry, and photophysics (PDF)

Crystallographic data of compound AG97 has been deposited in the Cambridge Crystallographic Data Centre (CCDC 1588151) (CIF)

AUTHOR INFORMATION

Corresponding Authors

*E-mail: cristiano.viappiani@unipr.it (C.V.).
*E-mail: ca.s@wwu.de (C.A.S.).

ORCID

Cristiano Viappiani: 0000-0001-7470-4770
Cristian A. Strassert: 0000-0002-1964-0169

DOI: 10.1021/acsami.8b02709
ACS Appl. Mater. Interfaces XXXX, XXX, XXX−XXX

Present Address

[#]Institute for Bioengineering of Catalonia (IBEC), The Barcelona Institute of Science Technology (BIST), Barcelona, Spain.

Notes

The authors declare no competing financial interest.

■ ACKNOWLEDGMENTS

Financial support from the Deutsche Forschungsgemeinschaft (DFG, EXC1003 Cells in Motion) is gratefully acknowledged.

■ REFERENCES

(1) Lee, L. C.-C.; Lau, J. C.-W.; Liu, H.-W.; Lo, K. K.-W. Conferring Phosphorogenic Properties on Iridium(III)-Based Bioorthogonal Probes through Modification with a Nitrone Unit. *Angew. Chem.* **2016**, *128*, 1058−1061.

(2) Lo, K. K.-W. Luminescent Rhenium(I) and Iridium(III) Polypyridine Complexes as Biological Probes, Imaging Reagents, and Photocytotoxic Agents. *Acc. Chem. Res.* **2015**, *48*, 2985−2995.

(3) McKenzie, L. K.; Sazanovich, I. V.; Baggaley, E.; Bonneau, M.; Guerchais, V.; Williams, J. A. G.; Weinstein, J. A.; Bryant, H. E. Metal Complexes for Two-Photon Photodynamic Therapy: A Cyclometallated Iridium Complex Induces Two-Photon Photosensitization of Cancer Cells under Near-IR Light. *Chem.—Eur. J.* **2017**, *23*, 234−238.

(4) Baggaley, E.; Sazanovich, I. V.; Williams, J. A. G.; Haycock, J. W.; Botchway, S. W.; Weinstein, J. A. Two-photon phosphorescence lifetime imaging of cells and tissues using a long-lived cyclometallated Npyridyl^Cphenyl^Npyridyl Pt(ii) complex. *RSC Adv.* **2014**, *4*, 35003−35008.

(5) Baggaley, E.; Botchway, S. W.; Haycock, J. W.; Morris, H.; Sazanovich, I. V.; Williams, J. A. G.; Weinstein, J. A. Long-lived metal complexes open up microsecond lifetime imaging microscopy under multiphoton excitation: from FLIM to PLIM and beyond. *Chem. Sci.* **2014**, *5*, 879−886.

(6) Magidson, V.; Khodjakov, A.; Sluder, G.; Wolf, D. E. Chapter 23-Circumventing Photodamage in Live-Cell Microscopy. *Methods in Cell Biology*; Academic Press, 2013; Vol. *114*, pp 545−560.

(7) Bartz, R. R.; Piantadosi, C. A. Clinical review: Oxygen as a signaling molecule. *Crit. Care* **2010**, *14*, 234.

(8) Sy, M.; Nonat, A.; Hildebrandt, N.; Charbonnière, L. J. Lanthanide-based luminescence biolabelling. *Chem. Commun.* **2016**, *52*, 5080−5095.

(9) Liu, S.; Zhang, Y.; Liang, H.; Chen, Z.; Liu, Z.; Zhao, Q. Time-resolved luminescence imaging of intracellular oxygen levels based on long-lived phosphorescent iridium(III) complex. *Opt. Express* **2016**, *24*, 15757−15764.

(10) Chen, Z.; Zhang, K. Y.; Tong, X.; Liu, Y.; Hu, C.; Liu, S.; Yu, Q.; Zhao, Q.; Huang, W. Phosphorescent Polymeric Thermometers for In Vitro and In Vivo Temperature Sensing with Minimized Background Interference. *Adv. Funct. Mater.* **2016**, *26*, 4386−4396.

(11) Liu, S.; Zhou, N.; Chen, Z.; Wei, H.; Zhu, Y.; Guo, S.; Zhao, Q. Using a redox-sensitive phosphorescent probe for optical evaluation of an intracellular redox environment. *Opt. Lett.* **2016**, *42*, 13−16.

(12) Yu, Q.; Gao, P.; Zhang, K. Y.; Tong, X.; Yang, H.; Liu, S.; Du, J.; Zhao, Q.; Huang, W. Luminescent gold nanocluster-based sensing platform for accurate H2S detection in vitro and in vivo with improved anti-interference. *Light: Sci. Appl.* **2017**, *6*, No. e17107.

(13) Zhang, K. Y.; Yu, Q.; Wei, H.; Liu, S.; Zhao, Q.; Huang, W. Long-Lived Emissive Probes for Time-Resolved Photoluminescence Bioimaging and Biosensing. *Chem. Rev.* **2018**, *118*, 1770−1839.

(14) Baggaley, E.; Weinstein, J. A.; Williams, J. A. G. Time-resolved emission imaging microscopy using phosphorescent metal complexes: taking FLIM and PLIM to new lengths. In *Structure and Bonding*; Lo, K. K.-W., Ed.; Springer, 2015; Vol. *165*, pp 205−256.

(15) Mydlak, M.; Mauro, M.; Polo, F.; Felicetti, M.; Leonhardt, J.; Diener, G.; De Cola, L.; Strassert, C. A. Controlling Aggregation in Highly Emissive Pt(II) Complexes Bearing Tridentate Dianionic N^N^N Ligands. Synthesis, Photophysics, and Electroluminescence. *Chem. Mater.* **2011**, *23*, 3659−3667.

(16) Allampally, N. K.; Strassert, C. A.; De Cola, L. Luminescent gels by self-assembling platinum complexes. *Dalton Trans.* **2012**, *41*, 13132−13137.

(17) Allampally, N. K.; Bredol, M.; Strassert, C. A.; De Cola, L. Highly Phosphorescent Supramolecular Hydrogels Based on Platinum Emitters. *Chem.—Eur. J.* **2014**, *20*, 16863−16868.

(18) Strassert, C. A.; Chien, C.-H.; Galvez Lopez, M. D.; Kourkoulos, D.; Hertel, D.; Meerholz, K.; De Cola, L. Switching On Luminescence by the Self-Assembly of a Platinum(II) Complex into Gelating Nanofibers and Electroluminescent Films. *Angew. Chem., Int. Ed.* **2011**, *50*, 946−950.

(19) Allampally, N. K.; Daniliuc, C.-G.; Strassert, C. A.; De Cola, L. Tuning the Structural and Photophysical Properties of Cationic Pt(II) Complexes Bearing Neutral Bis(triazolyl)pyridine Ligands. *Inorg. Chem.* **2015**, *54*, 1588−1596.

(20) Ewen, P. R.; Sanning, J.; Doltsinis, N. L.; Mauro, M.; Strassert, C. A.; Wegner, D. Unraveling Orbital Hybridization of Triplet Emitters at the Metal-Organic Interface. *Phys. Rev. Lett.* **2013**, *111*, 267401.

(21) Ewen, P. R.; Sanning, J.; Koch, T.; Doltsinis, N. L.; Strassert, C. A.; Wegner, D. Spectroscopic mapping and selective electronic tuning of molecular orbitals in phosphorescent organometallic complexes - a new strategy for OLED materials. *Beilstein J. Nanotechnol.* **2014**, *5*, 2248−2258.

(22) Bhowmick, D. K.; Stegemann, L.; Bartsch, M.; Allampally, N. K.; Strassert, C. A.; Zacharias, H. Controlled 2D-Confinement of Phosphorescent Pt(II) Complexes on Quartz and 6H-SiC(0001) Surfaces. *J. Phys. Chem. C* **2015**, *119*, 5551−5561.

(23) Sanning, J.; Ewen, P. R.; Stegemann, L.; Schmidt, J.; Daniliuc, C. G.; Koch, T.; Doltsinis, N. L.; Wegner, D.; Strassert, C. A. Scanning-Tunneling-Spectroscopy-Directed Design of Tailored Deep-Blue Emitters. *Angew. Chem., Int. Ed.* **2015**, *54*, 786−791.

(24) Sanning, J.; Stegemann, L.; Ewen, P. R.; Schwermann, C.; Daniliuc, C. G.; Zhang, D.; Lin, N.; Duan, L.; Wegner, D.; Doltsinis, N. L.; Strassert, C. A. Colour-tunable asymmetric cyclometalated Pt(ii) complexes and STM-assisted stability assessment of ancillary ligands for OLEDs. *J. Mater. Chem. C* **2016**, *4*, 2560−2565.

(25) Straub, L.; González-Abradelo, D.; Strassert, C. A. Oxygen-insensitive phosphorescence in water from a Pt-doped supramolecular array. *Chem. Commun.* **2017**, *53*, 11806−11809.

(26) Khmara, E. F.; Chizhov, D. L.; Sidorov, A. A.; Aleksandrov, G. G.; Slepukhin, P. A.; Kiskin, M. A.; Tokarev, K. L.; Filyakova, V. I.; Rusinov, G. L.; Smolyaninov, I. V.; Bogomyakov, A. S.; Starichenko, D. V.; Shvachko, Y. N.; Korolev, A. V.; Eremenko, I. L.; Charushin, V. N. Synthesis, structure, electrochemical and magnetic properties of 2,6-bis(5-trifluoromethylpyrazol-3-yl)pyridine and its NiII complexes. *Russ. Chem. Bull.* **2012**, *61*, 313−325.

(27) Galstyan, A.; Naziruddin, A. R.; Cebrián, C.; Iordache, A.; Daniliuc, C. G.; De Cola, L.; Strassert, C. A. Correlating the Structural and Photo-physical Features of Pincer Luminophores and Monodentate Ancillary Ligands in PtIIPhosphors. *Eur. J. Inorg. Chem.* **2015**, *2015*, 5822−5831.

(28) Comas-Barceló, J.; Rodríguez-Amigo, B.; Abbruzzetti, S.; Rey-Puech, P. d.; Agut, M.; Nonell, S.; Viappiani, C. A self-assembled nanostructured material with photosensitising properties. *RSC Adv.* **2013**, *3*, 17874−17879.

(29) Hong, Y.; Lam, J. W. Y.; Tang, B. Z. Aggregation-induced emission. *Chem. Soc. Rev.* **2011**, *40*, 5361−5388.

(30) Mei, J.; Leung, N. L. C.; Kwok, R. T. K.; Lam, J. W. Y.; Tang, B. Z. Aggregation-Induced Emission: Together We Shine, United We Soar! *Chem. Rev.* **2015**, *115*, 11718−11940.

(31) Riebe, S.; Vallet, C.; van der Vight, F.; Gonzalez-Abradelo, D.; Wölper, C.; Strassert, C. A.; Jansen, G.; Knauer, S.; Voskuhl, J. Aromatic Thioethers as Novel Luminophores with Aggregation-Induced Fluorescence and Phosphorescence. *Chem.—Eur. J.* **2017**, *23*, 13660−13668.

DOI: 10.1021/acsami.8b02709
ACS Appl. Mater. Interfaces XXXX, XXX, XXX−XXX

(32) Sinha, N.; Stegemann, L.; Tan, T. T. Y.; Doltsinis, N. L.; Strassert, C. A.; Hahn, F. E. Turn-On Fluorescence in Tetra-NHC Ligands by Rigidification through Metal Complexation: An Alternative to Aggregation-Induced Emission. *Angew. Chem., Int. Ed.* **2017**, *56*, 2785−2789.
(33) Schmidt, B.; Sankaran, S.; Stegemann, L.; Strassert, C. A.; Jonkheijm, P.; Voskuhl, J. Agglutination of bacteria using polyvalent nanoparticles of aggregation-induced emissive thiophthalonitrile dyes. *J. Mater. Chem. C* **2016**, *4*, 4732−4738.
(34) Mauro, M.; Aliprandi, A.; Septiadi, D.; Kehr, N. S.; De Cola, L. When self-assembly meets biology: luminescent platinum complexes for imaging applications. *Chem. Soc. Rev.* **2014**, *43*, 4144−4166.
(35) Rodríguez-Amigo, B.; Delcanale, P.; Rotger, G.; Juárez-Jiménez, J.; Abbruzzetti, S.; Summer, A.; Agut, M.; Luque, F. J.; Nonell, S.; Viappiani, C. The complex of hypericin with β-lactoglobulin has antimicrobial activity with potential applications in dairy industry. *J. Dairy Sci.* **2015**, *98*, 89−94.
(36) Jacobson, O.; Kiesewetter, D. O.; Chen, X. Albumin-Binding Evans Blue Derivatives for Diagnostic Imaging and Production of Long-Acting Therapeutics. *Bioconjugate Chem.* **2016**, *27*, 2239−2247.
(37) DeRosa, M.; Crutchley, R. J. Photosensitized singlet oxygen and its applications. *Coord. Chem. Rev.* **2002**, *233*−*234*, 351−371.
(38) Schneckenburger, H.; Wagner, M.; Weber, P.; Strauss, W. S. L.; Sailer, R. Autofluorescence Lifetime Imaging of Cultivated Cells Using a UV Picosecond Laser Diode. *J. Fluoresc.* **2004**, *14*, 649−654.
(39) Aubin, J. E. Autofluorescence of viable cultured mammalian cells. *J. Histochem. Cytochem.* **1979**, *27*, 36−43.
(40) Waters, J. C. Accuracy and precision in quantitative fluorescence microscopy. *J. Cell Biol.* **2009**, *185*, 1135−1148.
(41) Coelho, M.; Maghelli, N.; TTolić-Nørrelykke, I. M. Single-molecule imaging in vivo: the dancing building blocks of the cell. *Integr. Biol.* **2013**, *5*, 748−758.
(42) Sophie, B.; Alexandra, F.; Emerson, G.; Gary, S.; Nicolas, L.; Thomas, P.; Vincent, L. Time-gated cell imaging using long lifetime near-infrared-emitting quantum dots for autofluorescence rejection, 2014. *SPIE* **2014**, 8.
(43) Kodama, Y. Time Gating of Chloroplast Autofluorescence Allows Clearer Fluorescence Imaging In Planta. *PLoS ONE* **2016**, *11*, No. e0152484.
(44) Viappiani, C. Use of nonradiative decays of extrinsic fluorophores as structural and dynamical probes in protein environments: fluorescence quenching. *Biophys. Chem.* **1994**, *50*, 293−304.
(45) Hungerford, G.; Benesch, J.; Mano, J. F.; Reis, R. L. Effect of the labelling ratio on the photophysics of fluorescein isothiocyanate (FITC) conjugated to bovine serum albumin. *Photochem. Photobiol. Sci.* **2007**, *6*, 152−158.

DOI: 10.1021/acsami.8b02709
ACS Appl. Mater. Interfaces XXXX, XXX, XXX−XXX